

The Flinders University of South Australia

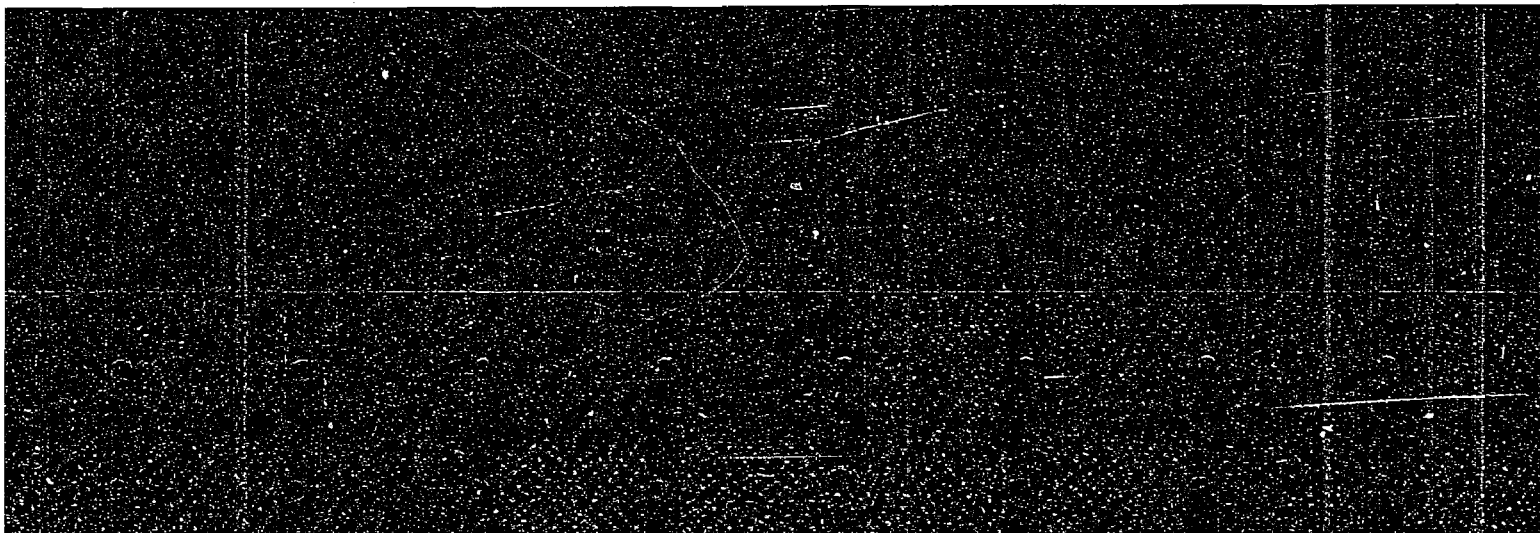
ELECTRONIC STRUCTURE OF MATERIALS CENTRE

Energy-momentum Spectroscopy of the Outervalence 3σ and 1π states of Hydrogen Fluoride: a reanalysis

R. Nicholson, I.E. McCarthy, E. Weigold and M.J. Brunger

ESM-125

March 1996



Electron Momentum Spectroscopy of the outervalence 3σ and 1π states of hydrogen fluoride: a reanalysis

R. Nicholson, I.E. McCarthy, E. Weigold* and M.J. Brunger

Physics Department, The Flinders University of South Australia, GPO Box 2100,
Adelaide, South Australia, Australia, 5001.

Abstract: We highlight and examine in detail a discrepancy that exists between the results of various single-channel and multiparameter electron momentum spectroscopy (EMS) studies into the outervalence states of hydrogen fluoride (HF). In an attempt to elucidate the nature of this problem and the disagreement that exists between the best available theoretical momentum distributions (MDs), as calculated in the plane-wave-impulse-approximation with wavefunctions at the near-Hartree-Fock limit, and the most accurate experimental MDs, we have adapted a method, originally applied to extract atomic orbital information from Compton profiles, to our 3σ and 1π experimental MDs. In addition we have also applied this technique to the $2s$ and $2p$ orbitals of neon, which is isoelectronic with HF, with the ramifications of the results of this investigation to HF also being outlined.

PACS #'s : 34.80Dp

* Permanent address: Institute of Advanced Studies, R.S. Phys. S.E., Australian National University, Canberra, ACT, Australia, 0200.

The purpose of this letter is to resolve a situation that has arisen over the analysis of the outervalence 1π and 3σ orbitals of HF by electron momentum spectroscopy (EMS). Previous experience with EMS of molecules has shown that the correct relationship of cross-section magnitudes between orbital manifolds is given by the plane-wave impulse approximation (PWIA), using orbital wave functions that correctly describe the shapes of the momentum distributions (MDs) up to a maximum momentum at least as high as 1 a.u. This could not be confirmed for HF by early experiments, because available self-consistent-field (SCF) orbitals could not reproduce the MD shapes. A recent experiment has raised questions over the measured relationships of 1π and 3σ MDs.

The original EMS investigation of HF by Brion *et al.* [1] at total energies of 400 and 1200 eV was a single-channel [2] coincidence experiment. Much-improved counting statistics were achieved by a 1500 eV multiparameter [2] investigation by Braidwood *et al.* [3]. The energy resolution 1.75 eV (FWHM) of [3] facilitated the deconvolution of the peaks in the energy distribution at the angle $\phi = 8^\circ$ in non-coplanar symmetric geometry [2], in comparison with the 2.1 eV (at 1200 eV) resolution of [1]. The 1π and 3σ peaks have separation energies 16.1 eV and 19.9 eV respectively.

The apparent inconsistencies are between different experimental measurements of the cross-section ratio for 3σ to 1π at $\phi = 8^\circ$, which is fundamental in setting the relative scale of the 3σ and 1π MDs. We note here that as the incident electron beam energies of Brion *et al.* [1] (1200 eV) and Braidwood *et al.* [3] (1500eV) were somewhat different, the observed momentum, at $\phi = 8^\circ$, will be slightly different in each case (0.68 a.u. compared to 0.73 a.u.). However this minor difference, which represents sampling the respective 3σ and 1π MDs at slightly different places, is not significant and does not diminish the argument that follows. The peak height ratio P of [3] is 0.48. The ratio of peak areas A was determined in [1] to be 0.55, where this value came from notes of the original analysis made by the authors of [1]. Braidwood *et al.* [3] electronically digitised the relevant data in fig. 3 of [1] and then fitted these data using a numerical least-squares deconvolution program. Each peak was represented by a Gaussian of width given by combining the instrumental width (2.1 eV) with the natural widths [4] of the 1π and 3σ states, which

are respectively 0.7 eV and 1.1 eV. The ratio A became 0.47 ± 0.04 , which we believe is the correct area ratio for [1]. The ratio P for [1] is 0.46. Note that the slightly larger width of the 3σ peak increases its area/peak ratio somewhat, in comparison with the 1π peak. The ratio of peak areas A for [3] was 0.49 ± 0.01 . The error here is much smaller than for the reanalysed result of [1] due to the improved statistical quality of the data.

In a recent single-channel experiment, also conducted at 1200 eV, Hollebhone *et al.* [5] found the value 0.56 for the peak area ratio A [6]. This result would necessarily have a larger error than for the multiparameter experiment [3]. Nevertheless we believe it is inconsistent with [3]. The peak height ratio P of [5] is 0.49 [6], consistent with [1] and [3]. A summary of this data for P and A of references [1], [3] and [5] is provided in table 1.

The peak area discrepancy must occur in the numerical processing of the energy spectra. First, different natural widths [6] for 1π are used for [3] and [5]. Estimates of natural widths come from the PES spectrum [4], which is reproduced in our fig. 1. The 1π state gives rise to four peaks. Braidwood *et al.* [3] digitised the 1π spectrum and numerically determined an envelope for the four peaks, arriving at the estimate 0.7 eV for the 1π natural width. If we base the estimate on the intense first peak, we obtain the result 0.2 eV of [5]. This ignores the less intense contributions from the other peaks and must be an underestimate. On the other hand, since the line profile is asymmetric, the estimate of [3] might weight the less-intense peaks too much. In fact this difference does not explain the peak area ratio discrepancy. We reanalysed the data of Braidwood *et al.* [3] using the extreme unphysical choices 0 eV and 1.3 eV for the 1π and 3σ natural widths and 1.75 eV for the instrumental width, obtaining $A = 0.51 \pm 0.01$, with a larger value of χ^2 than for [3]. Thus the ratio A is insensitive (to better than 4%) to the values employed for the natural widths. We believe that this is due to the broad instrumental width in both cases [1,3] and, in particular, to the significant broad tails of the instrumental response function.

We submit that evidence for the origin of the discrepancy in the ratio A can be found in fig. 1 of [5] where it is apparent that the real 1π flux at the leading edge of the first peak in their spectrum is not being taken into account in their fit. Presumably a similar

problem is also occurring at the tail of this peak. These tails are very important in deciding the ratio A , since the 1π tail under the 3σ peak is about twice as important as the 3σ tail under the 1π peak. We believe this to be the cause of the difference between the result of Braidwood *et al.* [3] and Hollebhone *et al.* [5] for A and thus the origin of the discrepancy between them. Further, we are confident that if Hollebhone *et al.* [5] were to make allowance for this in their analysis then, certainly to within their statistical uncertainties, all the three EMS measurements [1,3,5] would be reconciled.

In addition to the issues just described there has also been a discrepancy between the most reliable available theoretical MD calculations and experiment for the 1π and, to a lesser extent, 3σ momentum distributions [3,5,7,8]. Indeed evidence for the continued existence of this disagreement between theory and experiment is apparent in the most recent theoretical work of Duffy *et al.* [9], which included density functional theory (DFT) results. We note here that all their calculations were conducted within the plane-wave impulse approximation (PWIA) framework and that whilst the DFT approach [9] improved the level of agreement with experiment [3] for the 3σ to 1π cross section ratio (values at their respective peaks) over that obtained using Hartree-Fock wavefunctions, a significant discrepancy still remained. Consequently in an attempt to shed more light on the nature of this discrepancy we have adapted and applied a technique, originally developed by Schmider *et al.* [10] to extract atomic orbital information from Compton profiles, to our preferred 3σ and 1π MD data [3]. A brief description of this procedure is now given below along with some details of the PWIA and distorted-wave impulse approximation (DWIA) frameworks.

EMS measures the momentum profile $F_i(q)$ for states i of the residual ion in an ionisation reaction where the measured incident and two outgoing electron momenta are k_0 , k_A , k_B and

$$\mathbf{q} = \mathbf{k}_A + \mathbf{k}_B - \mathbf{k}_0. \quad (1)$$

For molecular targets in the kinematic range relevant to EMS there is a large body of

evidence [11,8] supporting the conclusion that the PWIA gives a quantitative relationship between the measurements and the target-ion structure, represented by the electronic ground states 0 of the target and i of the ion. The PWIA is

$$F_i(q) = \int d\hat{q} |\langle qi|0\rangle|^2, \quad (2)$$

where the structure amplitude is defined by

$$\langle qi|0\rangle = \langle k_A k_B i | 0 k_0 \rangle. \quad (3)$$

For atom targets in the region of 1 keV incident energy it is necessary to implement a refinement of the PWIA. The DWIA replaces the plane-wave states of the external electrons in (3) by the appropriate elastic-scattering states $\chi^{(\pm)}(\mathbf{k})$, thereby taking into account the effect of the rest of the system on the reaction. The DWIA is

$$F_i(q) = \int d\hat{q} |\langle \chi^{(-)}(\mathbf{k}_A) \chi^{(-)}(\mathbf{k}_B) i | 0 \chi^{(+)}(\mathbf{k}_0) \rangle|^2. \quad (4)$$

We will use the DWIA to describe the momentum profile in subsequent formalism, since the PWIA is a special case of it.

Further understanding of the structure amplitude comes from defining an appropriate set of target orbitals. $\langle qi|0\rangle$ is a one-electron function, the Dyson orbital. It is useful to define a normalised Dyson orbital α by the weak-coupling approximation,

$$\langle qi|0\rangle = (S_i^\alpha)^{1/2} \langle q|\alpha\rangle, \quad (5)$$

which assigns certain states i to an orbital manifold α , identified by identical shapes of the momentum profiles for all $i \in \alpha$, characteristic of the orbital α . S_i^α is the spectroscopic factor. Orbital manifolds are identified in all EMS experiments. They are due to the splitting of the one-hole ion state $\bar{\alpha}$, obtained by annihilating an electron in the target orbital α , which is occupied in the independent-particle configuration, by ion-state correlations. The correlations are described in a configuration-interaction representation by

admixture of determinantal configurations formed by excitations of particles and holes in the independent-particle configuration.

The momentum profile is

$$F_i(q) = S_i^\alpha \int d\hat{q} |\langle \chi^{(-)}(k_A) \chi^{(-)}(k_B) | \alpha \chi^{(+)}(k_0) \rangle|^2. \quad (6)$$

The intensity for states $i \in \alpha$ is proportional to S_i^α .

The weak-coupling approximation is confirmed experimentally by verifying two of its consequences. These are the spectroscopic sum rule for the manifold α

$$\sum_i S_i^\alpha = 1, \quad (7)$$

and the similarity of momentum profile shapes for the states $i \in \alpha$. In almost every known case the belief that the relative normalisation of states $i \in \alpha$ is given by the spectroscopic factor is confirmed by identifying enough states i to exhaust the sum rules (equation (7)) for different manifolds, which are then compared.

Until recently EMS analysis was performed in terms of orbitals obtained from self-consistent-field calculations of the target structure. In most cases these orbitals were sufficient to describe profile shapes, but glaring exceptions are known, for example the $1b_1$ manifold of water [12], which is essentially a one-state manifold but is not well described by a Hartree-Fock orbital. It is well described by a density-functional calculation [9].

Here we consider the experiment as a probe for the normalized Dyson orbital $\langle q | \alpha \rangle$ and we ask what function the experiment yields as an estimate of this orbital. The probe is described by the spherically-averaged impulse approximation, with appropriate weighting factors for experimental resolution. The estimate of the orbital is unravelled from the experimental data by a statistical inverse-scattering procedure that has been used previously [10] to extract atomic orbital information from Compton profiles. We determine the orbital shape and the partial sum of spectroscopic factors for a manifold α , represented by a normalisation factor G , by fitting EMS momentum profiles [13]. The experimental partial sum of momentum profiles $F_\alpha(q_\mu)$ at the set of data points

$\mu \equiv (\hat{k}_A, \hat{k}_B)$ is fitted by choosing a set θ of parameters to minimise the sum of weighted squares of the deviations.

$$F_\alpha(q_\mu) - G \int d\hat{q} \int d\hat{k} W_A(\hat{k}, \hat{k}_A) \int d\hat{k}' W_B(\hat{k}', \hat{k}_B) |\langle \chi^{(-)}(k) \chi^{(-)}(k') | \alpha \chi^{(+)}(k_0) \rangle|^2. \quad (8)$$

In spectroscopic experiments it is valid to consider the energies of the external electrons as well resolved, but to take into account angular resolution in the measurement of \hat{k}_A by integrating the momentum profile over a solid angle \hat{k} with a normalised weight factor $W_A(\hat{k}, \hat{k}_A)$ and similarly for \hat{k}_B . The weight of the point μ in the fit is the inverse of the variance of $F_\alpha(q_\mu)$.

The orbital α is represented as a linear combination of orthonormal basis orbitals β , whose symmetry is the same as α but whose principal quantum numbers are different.

$$|\alpha\rangle = \sum_{\beta} c_{\alpha\beta} |\beta\rangle; \quad \alpha, \beta = 1, \dots, n. \quad (9)$$

The fitting is constrained by the unitarity of the transformation matrix $c_{\alpha\beta}$, which ensures that the resulting orbitals are orthonormal. The unitarity constraint is achieved by parametrizing the coefficients with the set of Jacobi-type planar rotation matrices $R(\theta_j)$, which have the same dimension as $c_{\alpha\beta}$. The set θ of fitting parameters comprises the rotation angles θ_j and the normalization constraint G , which must be included because one overall normalization is not experimentally determined. Each fit determines n orbitals α , including the ones relevant to the data fitted.

The 3σ and 1π orbital manifolds of HF have provided an apparent exception to the rule that the PWIA gives correct relative normalisation of states in orbital manifolds [3,5,7]. Determination of their respective partial sums of spectroscopic factors has been hampered by the fact that their individual momentum profile shapes are not well described by the appropriate Hartree-Fock orbital. Figures 2 and 3 compare the PWIA momentum profiles, using the fitted 3σ and 1π orbitals and the corresponding basis orbitals, with our preferred experimental data [3]. Table 2 shows the fitting coefficients. The SCF basis orbitals were

calculated using the program GAMESS [14] with a STO-3G basis that yielded a total energy -99.958 a.u., compared with the experimental value [5] -100.460 a.u.

Considering figure 2 in more detail then it is immediately apparent that the present estimate of the normalized Dyson orbital (see table 2 for coefficients) provides a much better fit to the experimental 3σ MD data [3] than does that obtained using the basis 3σ orbital. Furthermore we note (see table 2) such a high quality fit was achieved using an orbital which allowed for about a 12% 1σ , 2σ and 4σ contribution. A very similar story for the 1π state is also found in figure 3. In this case the present orbital (see table 2 for coefficients), compared to that obtained by using the basis 1π orbital, again provides a far superior fit to the experimental 1π data [3]. Once again this excellent fit was achieved using an orbital which allowed for about a 11% 2π , 3π , 4π contribution. If we now calculate the ratio R of the normalisation constants G , determined in the fit to provide best agreement with experiment, then we find $R = 0.48 \pm 0.02$, a value in excellent agreement with that anticipated from the PWIA calculation ($R = 0.50$ because of the two-fold degeneracy of the 1π orbital), provided all the experimental flux for the respective 3σ and 1π orbitals was observed.

Clearly, we have found functions that estimate the normalized Dyson orbitals from the experimental 3σ and 1π MD data within the spherically-averaged PWIA framework. Relative error estimates are small. Braidwood *et al.* [3], when confronted with the discrepancy between their MDs and those obtained with the then best available orbitals in a PWIA calculation, looked to Ne, which is isoelectronic with HF, to try and glean further information on the reaction mechanism. For Ne we used the distorted-wave Born approximation (DWBA) in the analysis.

We have revisited Ne here, using the fitting technique [10] we discussed earlier, with the results for the coefficients $c_{\alpha\beta}$ being summarised in table 3 and the MDs being illustrated in figure 4 for the $2p$ state and figure 5 for the $2s$ state. Note that in figure 5 we have used the more recent Ne $2s$ results of Samardzic *et al.* [15], for the main $2s$ line of Ne at a binding energy of 48.46 eV, in our analysis. Occupied basis orbitals were obtained from a Hartree-Fock calculation [16]. Unoccupied basis orbitals were obtained from an effective

local potential [17] and they are orthogonalised to the occupied orbitals. It is apparent from the present analysis (see figures 4 and 5) that whilst the present wavefunctions do provide a somewhat better fit to the respective 2p and 2s experimental MD data, in both cases the fit obtained using the appropriate basis 2p and 2s orbitals, to within the uncertainty on the experimental data points, is still very good. This point is also borne out by expansion coefficients for the present 2p and 2s wavefunctions as given in table 3. In both cases the basis 2p and 2s orbital coefficients dominate in the experiment so that the respective wavefunctions are almost pure Hartree-Fock.

The present analysis, through the normalisation coefficients G , also derives a spectroscopic factor for the main 2s line of 0.913 ± 0.014 relative to 1 for the 2p manifold, in excellent agreement with the appropriate 2p and 2s S_p^α values reported in Samardzic *et al.* [15]. We have confirmed the earlier observation of Braidwood *et al.* [3] that to obtain a good fit to the experimental MD data, a distorted-wave framework must be employed in the atomic case. The HF analysis confirms earlier results that the PWIA is sufficient for MD shapes up to about 1 a.u. and also for relative normalisations of MDs for states of an orbital manifold.

Acknowledgements

One of us (R. Nicholson) thanks the Flinders University of South Australia for his scholarship, while M. Brunger acknowledges the Australian Research Council (ARC) for his QE2 Fellowship. This work was partially supported by an ARC Small Grant.

References

- [1] C.E. Brion, S.T. Hood, I.H. Suzuki, E. Weigold and G.R.J. Williams, *J. Elec. Spectrosc.* **21**, 71 (1980).
- [2] I.E. McCarthy and E. Weigold, *Rep. Prog. Phys.* **51**, 299 (1988).
- [3] S.W. Braidwood, M.J. Brunger, D.A. Kononov and E. Weigold, *J. Phys. B* **26**, 1655 (1993).
- [4] G. Bieri, L. Asbrink and W. von Niessen, *J. Elec. Spectrosc.* **23**, 281 (1981).
- [5] B.P. Hollebone, Y. Zheng, C.E. Brion, E.R. Davidson and D. Feller, *Chem. Phys.* **171**, 303 (1993).
- [6] C.E. Brion, private communication (1993).
- [7] E.R. Davidson, D. Feller, C.M. Boyle, L. Adamowicz, S.A.C. Clark and C.E. Brion, *Chem. Phys.* **147**, 45 (1990).
- [8] C.E. Brion, in "Correlations and Polarisation in Electronic and Atomic Collisions and (e,2e) Reactions", Institute of Physics. Conf. Series **122**, 171 (1992) (Bristol: IOP).
- [9] P. Duffy, D.P. Chong, M.E. Casida and D.R. Salahub, *Phys. Rev. A* **50**, 4707 (1994).
- [10] H. Schmider, V.H. Smith and W. Weyrich, *Z. Naturf. Forsch A, Phys. Phys. Chem. Kosmophys.* **48A**, 221 (1993).
- [11] I.E. McCarthy and E. Weigold, *Rep. Prog. Phys.* **54**, 789 (1991).
- [12] A.O. Bawagan, C.E. Brion, E.R. Davidson and D. Feller, *Chem. Phys.* **113**, 19 (1987).
- [13] R. Nicholson, PhD Thesis (1996), The Flinders University of South Australia, unpublished.
- [14] M.W. Schmidt, K.K. Baldrige, J.A. Boatz, J.H. Jensen, S. Koseki, M.S. Gordon, K.A. Nguyen, T.L. Windus and S.T. Elbert, *QCPE Bull.* **10**, 52 (1990).
- [15] O. Samardzic, S.W. Braidwood, E. Weigold and M.J. Brunger, *Phys. Rev. A* **48**, 4390 (1993).
- [16] E. Clementi and C. Roetti, *At. Data and Nucl. Data Tables* **14**, 177 (1974).
- [17] A.E.S. Green, D.L. Sellin and A.S. Zachor, *Phys. Rev.* **184**, 1 (1969).

Figure Captions

- Figure 1: Binding energy spectrum for HF from Brieri *et al.* [4], showing the 3σ and 1π intensities.
- Figure 2: A comparison of PWIA calculations for HF 3σ with experiment. (—) present orbital, (- - -) single 3σ orbital and (o) data of Braidwood *et al.* [3]. The present 1σ , 2σ , 3σ and 4σ orbitals were constructed from GAMESS 92 [14].
- Figure 3: A comparison of PWIA calculations for HF 1π with experiment. (—) present orbital, (- - -) single 1π orbital and (o) data of Braidwood *et al.* [3]. The present 1π , 2π , 3π and 4π orbitals were constructed from GAMESS 92 [14].
- Figure 4: A comparison of DWBA calculations of neon $2p$ with experiment. (—) present orbital, (- - -) single $2p$ Hartree-Fock orbital and (o) data of Braidwood *et al.*[3].
- Figure 5: A comparison of DWBA calculations for neon $2s$ with experiment. (—) present orbital, (- - -) single $2s$ Hartree-Fock orbital and (o) data of Samardzic *et al.* [15].

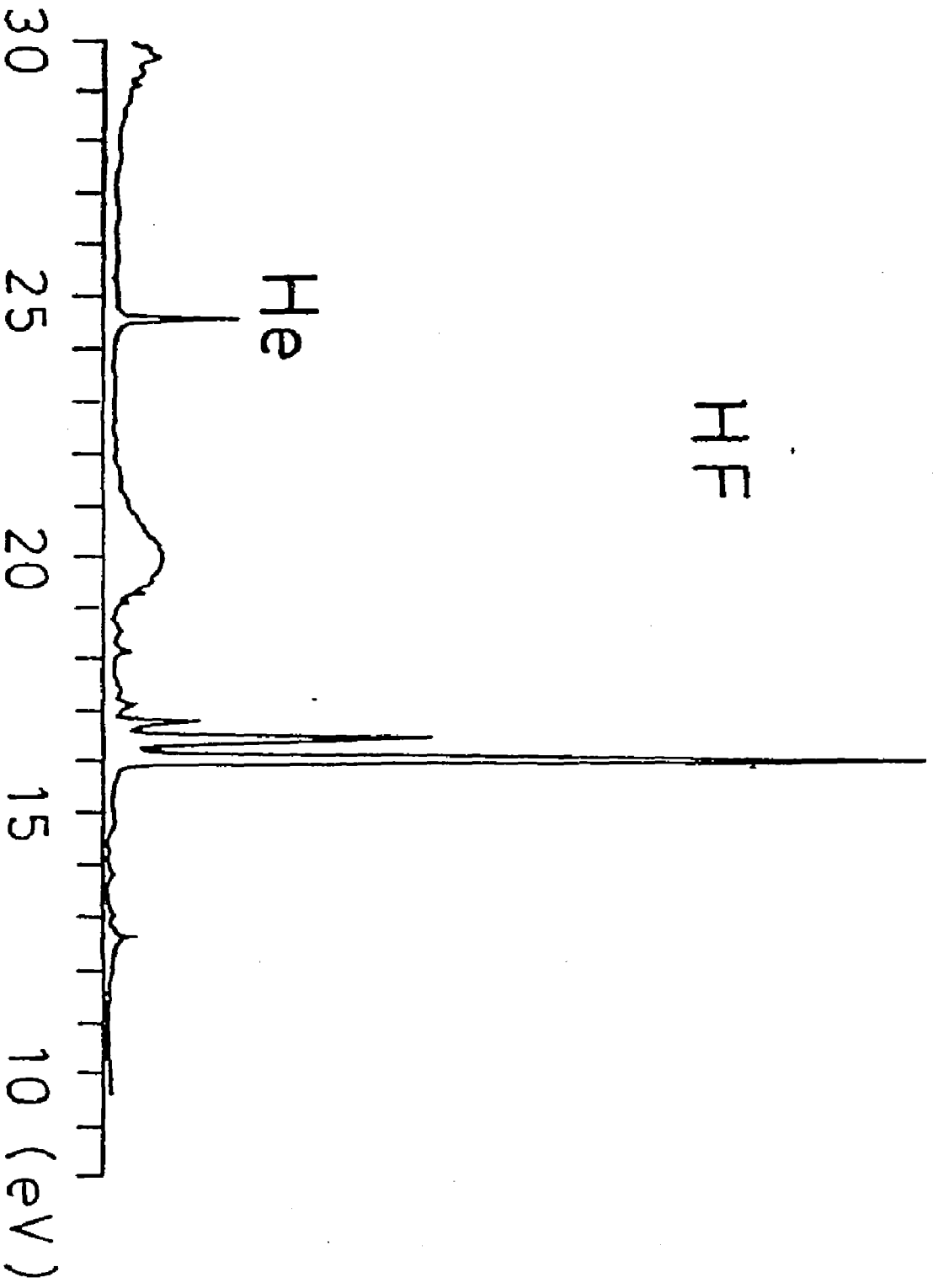


Fig. 1

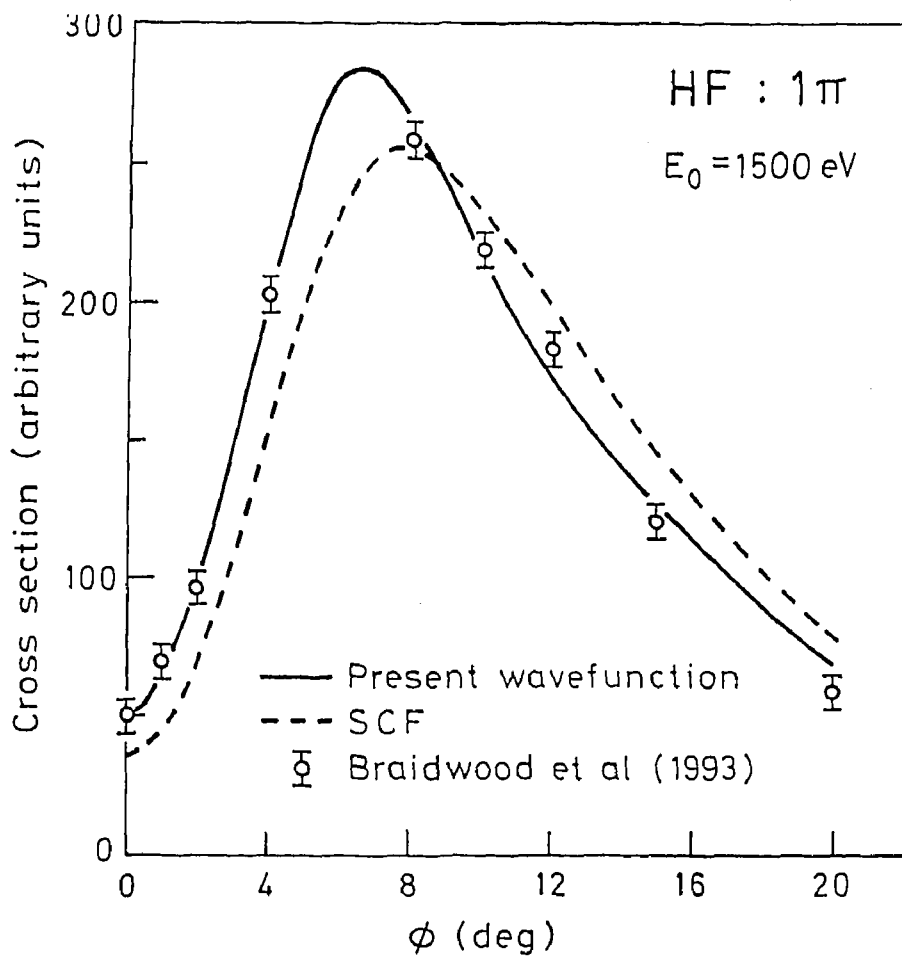


Fig. 3

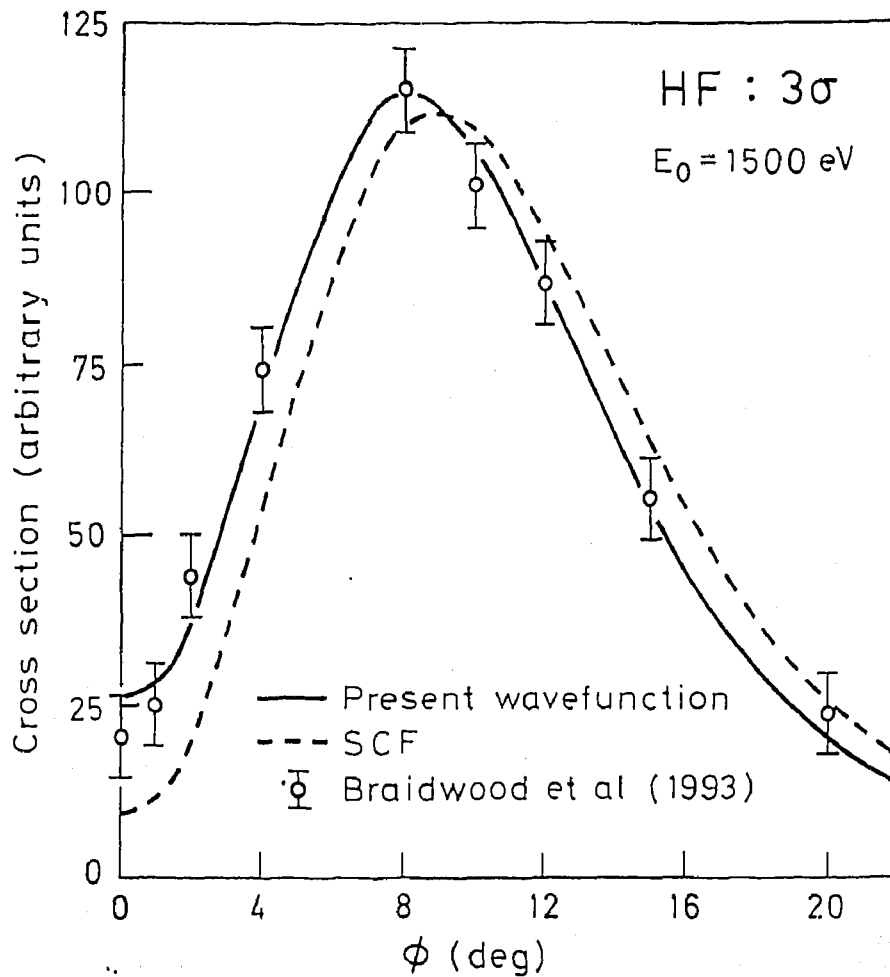


Fig. 2

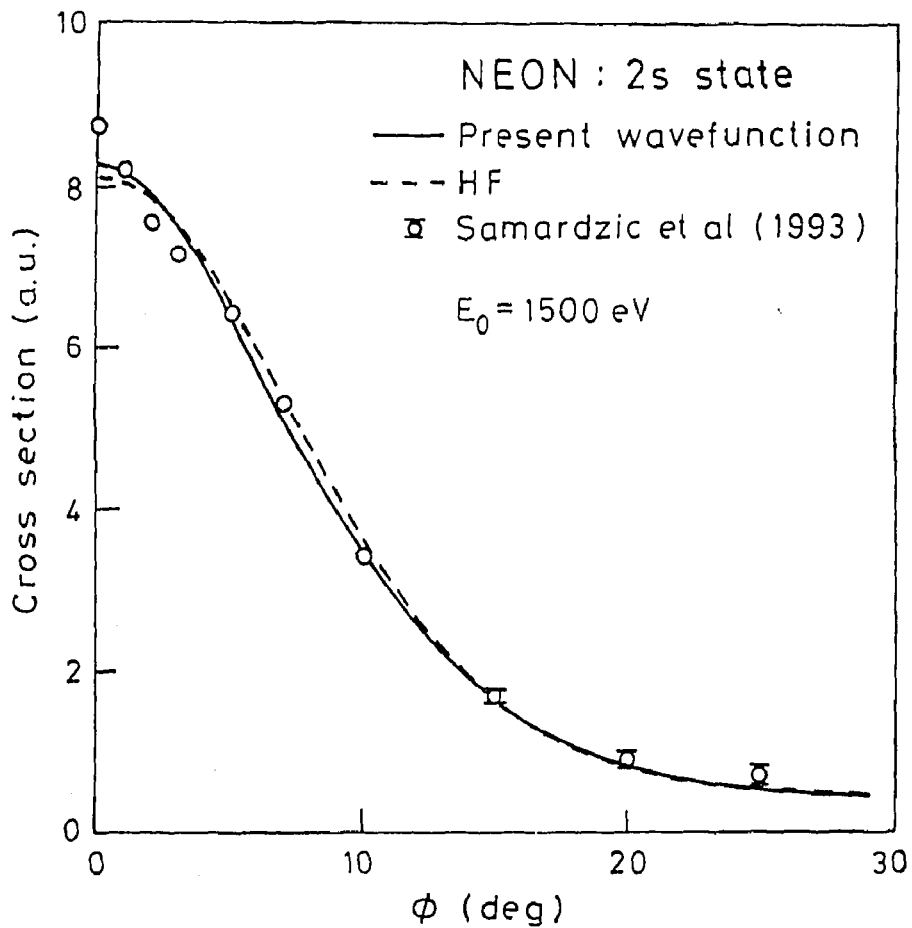


Fig. 5

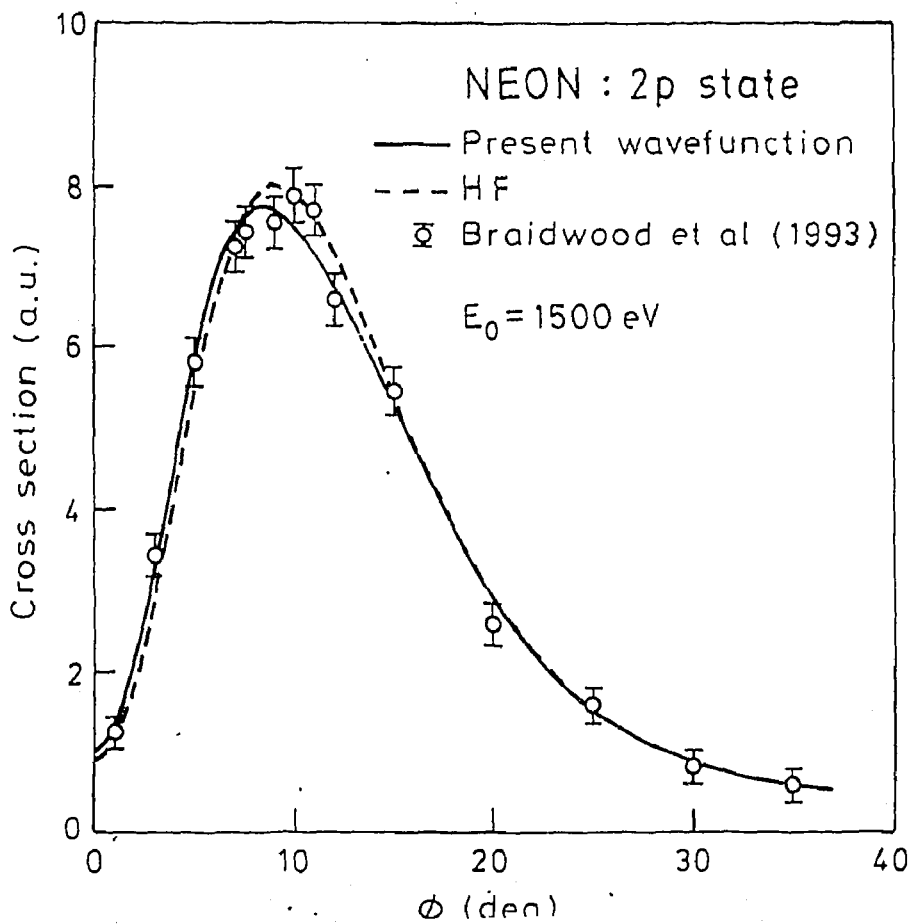


Table Captions

Table 1: Values of the 3σ to 1π peak height (P) and peak area (A) ratios at $\phi = 8^\circ$ of the available EMS studies on HF.

Table 2: Fitting coefficients and their standard deviations for the 1π and 3σ orbitals of HF.

Table 3: Fitting coefficients and their standard deviations for the 2s and 2p orbital manifolds of neon.

Table 1:

	P	A
Reference [1]	0.46	0.55
Reanalysed [1]	0.46	0.47 ± 0.04
Reference [3]	0.48	0.49 ± 0.01
Reference [3]	0.49	0.56

Table 2:

Basis	1π orbital coefficient	Basis	3σ orbital coefficient
1π	0.93940 ± 0.00900	1σ	0.32999 ± 0.11810
2π	0.17390 ± 0.01000	2σ	-0.06595 ± 0.00770
3π	0.24600 ± 0.03600	3σ	0.93782 ± 0.03940
4π	-0.01635 ± 0.02200	4σ	0.08520 ± 0.00540

Table 3:

Basis	$2s$ orbital coefficient	Basis	$2p$ orbital coefficient
$1s$	-0.02311 ± 0.06255	$2p$	0.99993 ± 0.00009
$2s$	0.99971 ± 0.00145	$3p$	0.00724 ± 0.00390
$3s$	-0.00099 ± 0.00045	$4p$	0.00908 ± 0.00628
$4s$	0.00739 ± 0.00102		